# Funneling of Low Energy Ion Beams *

W. Barth, A. Schempp
Institut für Angewandte Physik, J.W. Goethe-Universität
D-6000 Frankfurt 11, Postfach 111932, Germany

*Abstract*

Funneling is a way of increasing the brightness of ion beams by filling all rf-buckets of a rf-accelerator. Thus the higher current transport capability at higher energies and operating frequencies can be used. Funnel systems have been proposed e.g. for HIIF type drivers and spallation neutron sources. Results of numerical simulations and funneling experiments at Frankfurt will be reported, where a set up with a 50 keV proton beam and a rf deflector is investigated to study especially emittance growth effects in funneling lines.

## 1. Introduction

The idea of funneling two or more beams together is an important way to reduce the cost and complexity of accelerators designed to produce intense beams with high brightness. In principle the ion beams e.g. from two identical low-frequency structures are funneled into a single high frequency accelerator in such a way that every bucket of the high-frequency accelerating field is filled. For a simple two channel line the two beams have to be bunched and accelerated in identical rf-accelerators at the frequency $f_0$, with a phase shift of 180 degrees between them (Fig. 1.).

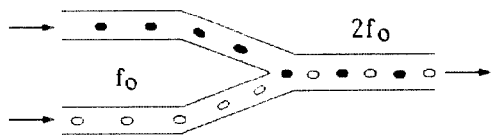


Fig. 1. Principle of a two channel funneling line.

A perfect funneling line doubles the beam current and the transverse brightness at twice the frequency without any emittance growth. Applications of funneling could include accelerators for heavy ion inertial fusion (HIIF) or SNQ-type accelerators [1].

Funneling in a RFQ-like structure is a possibility for beam merging at low energies [2]. For high energies funneling with discrete elements is more flexible but also more expensive [3], [4]. A beam line, with a single leg of a prototype 5-MeV funnel for light ions was sucessfully tested [5].

* supported by BMFT under contract no. 06 OF186 I

## 2. Defunneling

Because of the experimental difficulties in building to identical accelerators , we investigated funnel structures at first in a different way: one bunched ion beam is divided in two displaced beams with 180° phaseshift and half repetition frequency. Most of the physics issues, which arise in a real funnel section, are investigable, e.g. the design and operating of the rf deflector - the neuralgic point of every funnel - can be optimized. Furthermore we can use the defunnel line itself as an injection system for a funnel experiment, because the two output beams of the defunnel line have all the required properties.

## 3. Field Calculations

The deflector is a plate capacitor of length L symmetrically placed around the z-axis (the axis of the injection accelerator) with a time varying electric field: $E_x(t) = A \sin(\omega t - \varphi)$. If we neglect fringing fields at first, the electric field inside the deflector has only a homogenous and time-dependent x-component. Besides the peak deflecting amplitude A, such an ideal deflector is described by its length L, the frequency $\omega$ and the phase $\varphi$.

Considering fringing fields (x-component), A is replaced by a term A(z), which depends on z. We used a version of the SLAC166 simulation code [6,7] to calculate the potential $\Phi(x,z)$ in the deflector. From this the electric field component $E_x(z)$ on axis is obtained.

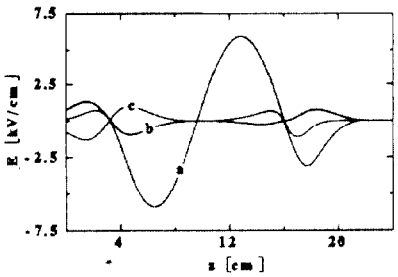


Fig. 2. The deflecting field component $E_x(x,z)$ (a) and the corresponding longitudinal field component $E_z(x,z)$ (b) calculated with a potential grid $\Phi(x,z)$; in addition $E_z$ for a particle in the center of an adjacent bunch (c).

In a next step the dependence of $E_x$ on x and also the accelerating or decelerating field com-

ponent $E_z(x,z)$ was investigated. For that purpose we used the complete potential grid calculated by SLAC166. The actual field components are obtained by using the actual coordinates ($x_{act}$, $z_{act}$) of the particle (an example is shown in Fig. 2). This is done for every particle in the multiparticle simulations.

## 4. Experimental Set up

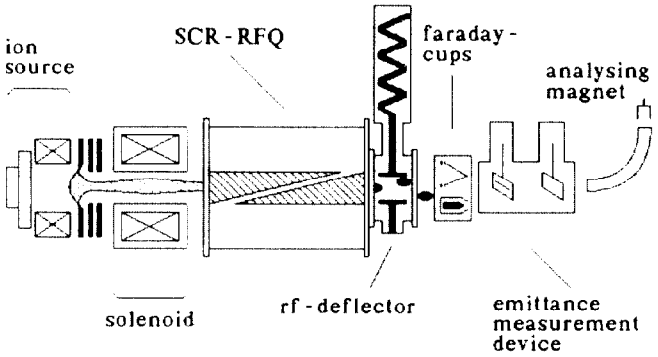


Fig. 3. The experimental set up of the defunnel line.

| | SCR-RFQ | RF-Defl. |
|---|---|---|
| f (MHz) | 50 | 25 |
| Voltage (kV) | 9 max. | 40 |
| Rp-value (kΩ) | 180 | 290 |
| Qo-value | 4500 | 850 |
| $T_{in}$ (keV) | 6.5 | 50 |
| $T_{out}$ (keV) | 50 | 50 |
| Aperture (mm) | 6-4.5 | 42 or 28-48 |
| Modulation | 1.16-1.88 | - |
| $\varphi_s$ (°) | 60-30 | - |
| $\varphi_{ot}$ (°) | 45 | - |
| Length (cm) | 55 | 10 or 16 |
| Cell number (βλ) | 32 | 0.5 or 1 |
| $I_{max}$ (mA) | 4.2 | - |
| Displacement (mm) | - | 25 |

Tab. 1. The parameters of the defunnel experiment.

The experimental set up of the defunnel line is shown in Fig. 3. The injection system of the defunnel element consists of a plasma beam ion source [8], an extraction system, and a Split Coaxial-RFQ with rod electrodes [9].

With hydrogen operation the plasma beam ion source supplies a proton fraction of 90% at a max. beam current of 6 mA. The ions are extracted with an accel/decel-system at an extraction voltage of 6.5 keV. We use a solenoidal lense [10] to match the ion source beam to the 50 MHz SCR-RFQ. The SCR-RFQ accelerates the $H^+$-beam from 6.5 keV to 50 keV.

In the adjacent defunnel element (25 MHz) the beam is divided into parallel beams. The deflector is part of a helix-λ/4-resonator. Thus the cavity of the deflector can be very small. Three electrode geometries were tested (with different length l): $l = \beta\lambda$, $l = \beta\lambda$ with a gapwidth of 28 mm at the beginning and 48 mm at the end, $l = \beta\lambda/2$.

For diagnostic we use faradaycups (beam current, bunchstructure), an emittance measurement device [11] and an analysing magnet for energy spectra. The parameters of the defunnel system are summarized in Tab. 1.

## 5. Experimental Results

The horizontal displacement x from the z-axis, the angle x' and the horizontal emittance growth were measured as a function of the relative rf-phase. Fig. 4. shows (x,x') for all possible rf-phases. The agreement between measurement and simulations is excellent. The beam deflection scales with deflection voltage as expected. The application of the βλ- and the βλ/2-electrodes is efficient to get two parallel beams behind the defunnel element (x'=0). A maximum of displacement (at the same deflector voltage) was obtained by the special βλ-electrodes.

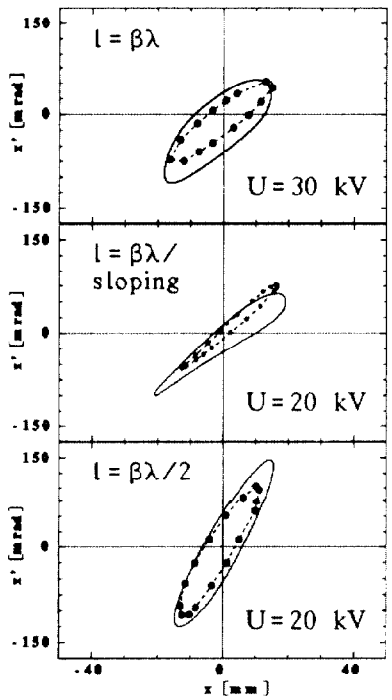


Fig. 4. x,x' as a function of the relative rf-phase φ.

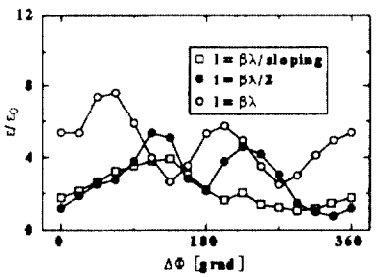


Fig. 5. The emittance growth as a function of the relative rf-phase φ at a beam current I of 0.1 mA. The deflector voltage is the same as in Fig. 4.

The emittance growth (Fig. 5.) shows a dependence on the relative rf-phase which is determined by the asymmetric field distribution inside the rf deflector. The special $\beta\lambda$-geometry is excellent suited to minimize emittance growth behind the deflector. With the rf deflector set to the optimized phase ($90^{o}$ for min. average emittance growth) the measured displacement between the centers of the beams was 20 mm at a deflection voltage of 40 kV.

In Fig. 6. a comparison between the calculated and measured x,x'-emittance for the two output beams is shown. There are two effects which are confirmed by the experiment: an offset in angle, which depends on the rf voltage (but independent on rf-phase) and moreover a rotation of the emittance, which is deflected to the right side. Both can be explained by the asymmetric field distribution. As an example Fig. 7. shows a 3d-represantation of the x,x'-emittance at deflector voltage of 20 kV.

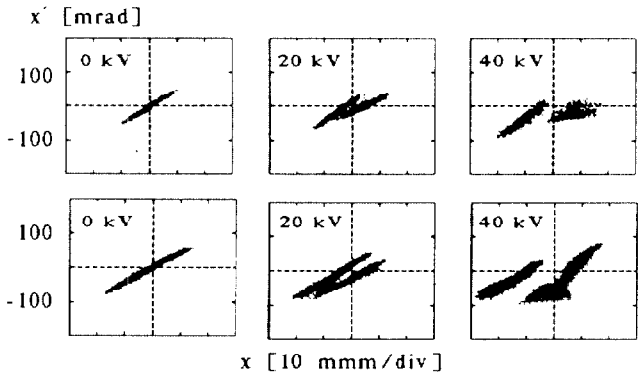


Fig. 6. The x,x'-emittance as a function of the deflector voltage. The results of the simulations are shown on the top, those of the experiments on the bottom (I=1.2 mA).

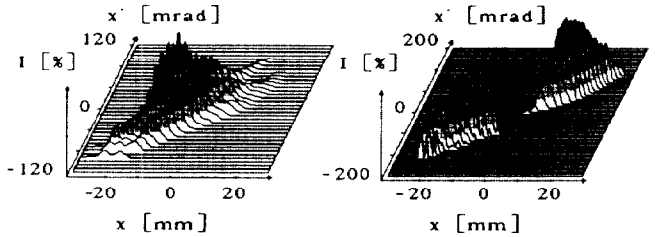


Fig. 7. The 3d x,x'-emittance at a deflector voltage of 20 kV. On the left: $\Delta x' = 0$ ($l = \beta\lambda$), on the right: $\Delta x_{max}$ ($l = \beta\lambda$/sloping). The beam current I is 1.2 mA.

The bunchlength depends on the relative rf-phase as seen in Fig.8. Because of the short total length of the rf deflector the bunchlength of the deflector with $\beta\lambda/2$-electrodes is minimized.

Fig. 9 illustrates the difference of neighbouring bunches. The beam which is deflected to the left side is very well bunched, in contrast the other one is debunched. The value of the deflecting component of the rf-field is nearly independent on the direction of the deflection. But the longitudinal field component $E_z(x,z)$, as seen in Fig. 2., shows a significant difference for a bunch deflected to the left or to the right side.

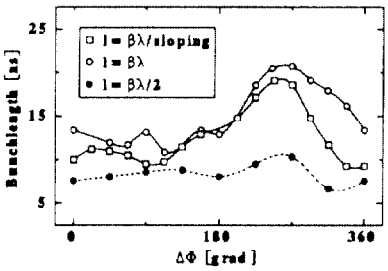


Fig. 8. The bunchlength as a function of the relative rf-phase (I=1.2 mA), same rf voltage as in Fig. 4.

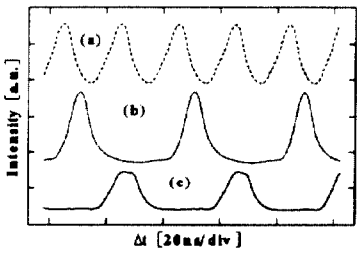


Fig. 9. The bunch structure of a drifting beam (a), a beam deflected to the left side (b) (right side (c)). The rf voltage is 20 kV ($l = \beta\lambda/2$; $\Delta x_{max}$); I=1.2 mA.

As a conclusion, the use of the defunnel experiments were successful. The dependence of beam deflection, horizontal emittance growth and bunchstructure on deflection amplitude and relative rf-phase, as well as effects of asymmetries were predicted by the simulations.

## 6. Acknowledgements

The authors thank all colleagues to their help, especially G. Hausen and I. Müller. All calculations were done at the HRZ/Frankfurt.

## 7. References

[1] T.P. Wangler et. al., Linac, LA-12004-C, 1990, p.548.
[2] R.H. Stokes, G.N. Minerbo, IEEE-NS-32, 1985, p.2593
[3] K. Bongardt, D. Sanitz, HIIF, GSI 82-8, p.224, 1982
[4] J.F. Stovall et. al., NIM A278, 1989, p 143
[5] K.F. Johnson et. al., Linac, LA-12004-C, 1990, p.701.
[6] W.B. Herrmannsfeldt, SLAC Rep. 166, 1973
[7] W. Sinz, thesis, Univ. Frankfurt, 1986.
[8] K. Langbein, EPAC, Rome, 1988, p.1228.
[9] P. Leipe, thesis, Univ. Frankfurt, 1989.
[10] A. Müller-Rentz, dipl. thesis, Univ. Frankfurt, 1986.
[11] G. Riehl, thesis, Univ. Frankfurt, (in prep.).
[12] W. Barth, A. Schempp, GSI-Rep. 91-27, p.44, 1991
[13] W. Barth, A. Schempp, PAC 91, San Francisco, 1991.